

# 铝合金激光清洗表面形貌变化的实验研究及工艺参数优化

李宇强<sup>1</sup>, 郭玲玉<sup>1</sup>, 蒋平<sup>1\*</sup>, 耿韶宁<sup>1</sup>, 王春明<sup>2</sup>, 高嵩<sup>1</sup>, 韩楚<sup>1</sup>

<sup>1</sup>华中科技大学机械科学与工程学院, 湖北 武汉 430074;

<sup>2</sup>华中科技大学材料科学与工程学院, 湖北 武汉 430074

**摘要** 铝合金密度低、比强度高,是理想的新能源汽车车身材料,但表面氧化层的存在严重影响焊接质量。激光清洗是一种基于脉冲激光的热烧蚀作用去除表面氧化层的方法,具有非接触、可控性好等优点。激光清洗处理会使铝合金表面形貌发生明显变化,对后续加工(如焊接、涂装等)有显著影响。研究了 6061 铝合金激光清洗表面形貌的变化规律,并建立了表面自然氧化层的激光清洗工艺窗口;基于此窗口,构建了 6061 铝合金表面粗糙度变化函数模型,对工艺参数进行优化。结果表明:平均功率影响凹坑形貌的变化尺寸,进而改变表面粗糙度,随着功率由 15 W 升高至 75 W,粗糙度逐渐增大;扫描速度和线间距影响相邻凹坑的搭接形貌,进而改变粗糙度,随着扫描速度由 2000 mm/s 升高至 6000 mm/s,线间距由 0.02 mm 升高至 0.06 mm,粗糙度先增大后减小。6061 铝合金自然氧化层的激光清洗工艺窗口的参数为:平均功率为 30~60 W,扫描速度为 3000~5000 mm/s,线间距为 0.03~0.05 mm,采用此窗口的工艺参数进行激光清洗后,粗糙度最大为 1.584  $\mu\text{m}$ 。

**关键词** 激光技术; 激光制造; 激光清洗; 铝合金; 表面形貌; 粗糙度; 工艺参数优化

中图分类号 TN249

文献标志码 A

doi: 10.3788/CJL202148.2202016

## 1 引言

铝合金具有密度低、比强度高特点,被广泛应用于航空航天、汽车制造等领域<sup>[1-2]</sup>。铝合金表面容易生成氧化层,而氧化层会严重影响焊接质量<sup>[3-4]</sup>,因此亟需一种高效的清除技术。激光清洗方法利用脉冲激光的热烧蚀作用去除铝合金表面的氧化层。与传统清洗方法(如机械打磨、化学清洗等)相比,激光清洗在清除效果、工艺柔性等方面具有明显的优势<sup>[5]</sup>,逐渐成为了常用的工业清洗手段。

激光清洗处理会明显改变铝合金的表面形貌和粗糙度,从而严重影响焊接、涂装等后续加工。Yousaf 等<sup>[6]</sup>发现激光清洗后,铝合金表面会形成“火山坑”形状的凹坑形貌,且随着激光能量的升高,“火山坑”形貌尺寸先增大后减小。Zheng 等<sup>[7]</sup>根据激光作用机理和凹坑形貌特征,将激光辐照区域划

分为烧蚀区、熔化区、沉积区等 5 部分,并对各区域内的形貌变化机制进行了理论分析。Zhu 等<sup>[8]</sup>发现激光清洗能够显著提升 5A12 铝合金的表面粗糙度,但并未系统地阐释粗糙度的变化规律。Shi 等<sup>[9]</sup>发现激光清洗处理能够在铝合金表面形成 9~30  $\mu\text{m}$  厚的硬化层,该硬化层轻微地提高了基材的拉伸性能和弯曲性能。Zhang 等<sup>[10-11]</sup>建立了材料热力学模型,认为蒸发压力引起的冲击效应导致了凹坑形貌的形成。Liu 等<sup>[12-14]</sup>通过工艺实验发现采用适当的工艺参数清洗后,金属合金表面的粗糙度可以得到一定程度的降低,但并未解释粗糙度降低的原因。文献<sup>[15-17]</sup>通过元素测试获取了铝合金激光清洗的工艺窗口,但并未结合工业应用进一步优化工艺参数。

综上所述,一些学者仅对比了激光清洗前后铝合金表面形貌的差异,但并未系统地解释形貌变化和粗糙度变化的原因。本文以 6061 铝合金为对象,

收稿日期: 2021-05-31; 修回日期: 2021-06-17; 录用日期: 2021-06-30

基金项目: 国家自然科学基金(52075201, 51861165202)、中国博士后科学基金(2020M682407)、数字制造设备与技术国家重点实验室开放项目(DMETKF2018001)

通信作者: \*jiangping@hust.edu.cn

开展工艺实验。探究了激光清洗工艺参数、表面形貌和粗糙度的关系,建立了 6061 铝合金表面自然氧化层的激光清洗工艺窗口。基于此窗口,构建了 6061 铝合金粗糙度变化函数模型,并对工艺参数进行优化,为激光清洗调控铝合金表面形貌提供理论基础和工艺指导。

## 2 实验方法

### 2.1 实验设备与材料

使用最大功率为 100 W 的脉冲激光器(YDFLP-100-LM1)进行激光清洗实验,X 振镜和 Y 振镜的高速运动将激光能量以二维排布的形式作用于材料表面,激光清洗设备结构如图 1 所示。激光波长为 1064 nm,最大单脉冲能量为 1.5 mJ,光斑直径  $D$  为 70  $\mu\text{m}$ 。固定脉宽为 100 ns,重复频率为 100 kHz。

表 1 6061 铝合金各组分的质量分数

Table 1 Mass fraction of each component for 6061 aluminum alloy

Element	Cu	Mn	Mg	Zn	Cr	Ti	Si	Fe	Al
Mass fraction /%	0.15–0.4	0.15	0.8–1.2	0.25	0.04–0.35	0.15	0.4–0.8	$\leq 0.7$	Balance

### 2.2 实验步骤

采用单因素实验研究平均功率  $P$ 、扫描速度  $v$  和线间距  $l_y$  对激光清洗效果的影响。平均功率影响激光能量的大小,过小的功率无法去除表面氧化层,而过大的功率会导致二次氧化。扫描速度和线间距分别影响横向光斑间距  $l_x$  和纵向光斑间距,如图 2 所示。

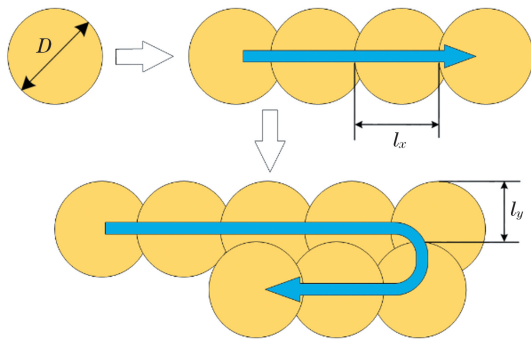


图 2 激光清洗过程中光斑排布示意图

Fig. 2 Schematic diagram of spot arrangement during laser cleaning

扫描速度与横向光斑间距的关系为

$$l_x = \frac{v}{f}, \quad (1)$$

式中: $f$  为重复频率。

激光清洗前,采用线切割方法将铝合金板材切成 10 mm × 10 mm × 2 mm 的方形试样,并用酒精

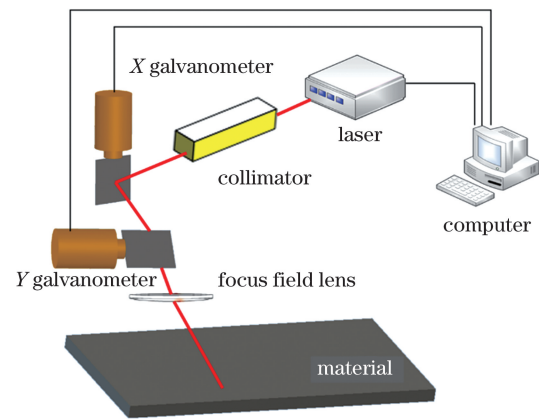


图 1 激光清洗设备结构

Fig. 1 Structure of laser cleaning equipment

使用的厚度为 2 mm 的 6061 铝合金具有密度低、比强度高优点,在新能源汽车车身中得到了广泛应用,化学成分如表 1 所示。

擦拭表面。激光清洗后,采用扫描电子显微镜(FEI Sirion 200 型)对表面形貌进行表征,采用能谱仪(EDS)对表面元素含量变化进行测试,采用超景深三维显微镜(OLYMPUS DSX 510 型)测试表面粗糙度  $S_a$  的变化。

### 2.3 工艺参数优化方法

激光清洗会明显改变铝合金的表面形貌和粗糙度。相关研究人员发现高粗糙度会增大表面对激光的吸收率以及涂层与基材间的附着力<sup>[18-20]</sup>。考虑到激光清洗是激光焊接和涂装的预处理手段,在建立的激光清洗工艺窗口内,基于响应面分析方法,以能达到的最大粗糙度为目标对工艺参数进行进一步优化。响应面分析法是用于处理多变量问题建模和优化的统计方法,并逐渐成为工程设计优化最有效的工具之一<sup>[21-22]</sup>。

对于一个响应量  $y$ ,可构造一个多项式近似函数表达其与一系列变量  $x$  的关系:

$$y \approx f(x). \quad (2)$$

以二阶响应面模型为例,响应面近似函数为

$$\hat{y} = \alpha_0 + \sum_{i=1}^n \alpha_i x_i + \sum_{i=n+1}^{2n} \alpha_i x_i^2 + \sum_{i=1}^{n-1} \sum_{j=i+1}^n \alpha_{ij} x_i x_j, \quad (3)$$

式中: $n$  为变量  $x$  的个数; $\alpha_0$ 、 $\alpha_i$  和  $\alpha_{ij}$  分别为常数项系数、一次项系数和二次项系数。

### 3 实验结果和讨论

#### 3.1 6061 铝合金激光清洗后表面形貌变化分析

图 3 为不同平均功率激光清洗后铝合金的表面形貌,扫描速度为 4000 mm/s,线间距为 0.04 mm。当功率为 15 W 时,铝合金表面仅形成小的凹坑形貌。由于激光能量低,表面氧化层厚度不均,大部分区域并没有出现相同尺寸的烧蚀凹坑。激光清洗后的表面形貌与单个脉冲激光辐照后的形貌密切相关。文献[23]指出脉冲激光处理过程中,材料表面熔池的流动受反冲压力、重力等作用。图 4 为激光清洗过程中

铝合金熔池的流动。金属表面在激光热作用下形成熔池区域,熔池受热形成蒸汽团。金属蒸气的喷发对表面熔池产生巨大的反冲压力作用,流体沿着固液界面向熔池边缘运动,最终形成中部凹陷、四周凸起的“环形山”形貌。当功率为 30,45,60 W 时,从图 3 中可以看到排布规律的凹坑形貌,并且相邻的凹坑互相搭接。随着功率的升高,搭接形貌逐渐失稳。当功率升至 75 W(单脉冲能量为 0.75 mJ)时,金属飞溅现象严重,无明显的凹坑搭接痕迹,这是因为激光能量过大导致热烧蚀作用剧烈,金属流体在巨大的反冲压力作用下大量飞溅,最终破坏了凹坑搭接形貌。

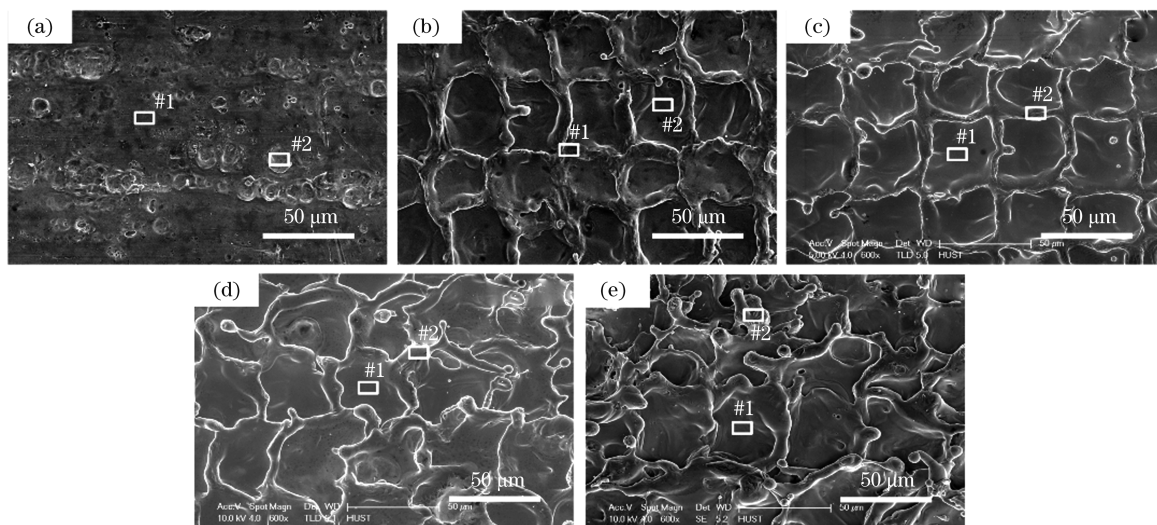


图 3 不同功率激光清洗后 6061 铝合金的表面形貌。(a) 15 W;(b) 30 W;(c) 45 W;(d) 60 W;(e) 75 W

Fig. 3 Surface morphology of 6061 aluminum alloy after laser cleaning with different power. (a) 15 W; (b) 30 W; (c) 45 W; (d) 60 W; (e) 75 W

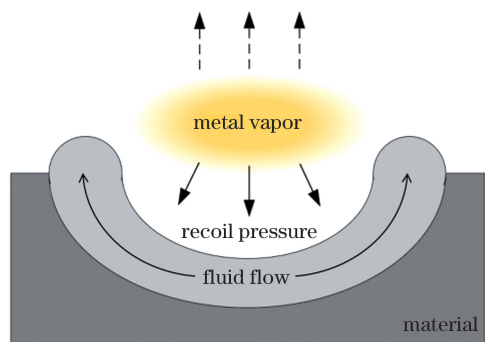


图 4 激光清洗过程中熔池的流动

Fig. 4 Flow of molten pool during laser cleaning

表面形貌的变化会显著影响粗糙度。线粗糙度基于线轮廓法评定粗糙度,用于表征表面一维轮廓的粗糙程度;面粗糙度基于区域形貌评定粗糙度,用于表征物体表面二维形貌的粗糙程度。面粗糙度更适合表征激光清洗后材料表面粗糙度的变化情况。图 5 为表面粗糙度随平均功率的变化情况,测量结果误差在 0.01  $\mu\text{m}$  以内。从图中可以看出,随着功

率由 15 W 升至 75 W,粗糙度  $S_a$  由 0.608  $\mu\text{m}$  增大至 1.636  $\mu\text{m}$ ,但增大的趋势逐渐变缓。结合图 3 和图 5,可以把铝合金表面形貌随功率的变化过程分为 4 个阶段。当功率为 15 W 时,如图 6(a)所示,由于激光热作用小,凹坑形貌的宽度  $d$  和深度  $h$  较小,相邻凹坑并没有重叠,表面仍有大部分平坦区

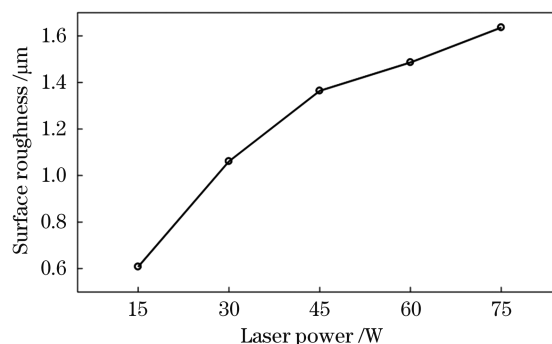


图 5 不同功率激光清洗后铝合金表面粗糙度

Fig. 5 Surface roughness of 6061 aluminum alloy after laser cleaning with different power

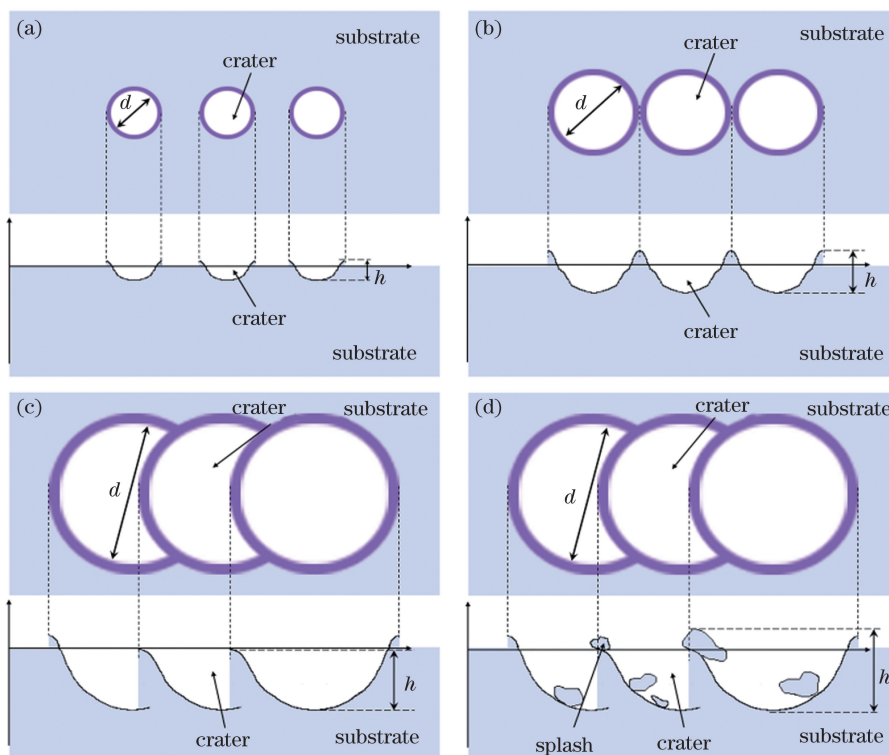


图 6 铝合金表面形貌随激光功率的变化过程。(a)~(d)阶段 1~阶段 4

Fig. 6 Change process of aluminum alloy surface morphology varying with laser power. (a)~(d) Stage 1~stage 4

域,此时的粗糙度  $S_a$  仅为  $0.608 \mu\text{m}$ 。功率升至  $30 \text{ W}$  时,如图 6(b)所示,单个凹坑形貌尺寸随之增大,相邻的凹坑互相搭接,表面大部分区域被凹坑覆盖,粗糙度  $S_a$  增大至  $1.061 \mu\text{m}$ 。当功率升至  $45 \text{ W}$  和  $60 \text{ W}$  时,如图 6(c)所示,凹坑宽度的增大导致相邻凹坑形貌具有一定的重叠,激光功率的升高和相邻光斑的热积累导致凹坑的深度继续加深,粗糙度

$S_a$  大幅增大至  $1.364 \mu\text{m}$  和  $1.486 \mu\text{m}$ ,由于光斑重叠率的限制,粗糙度增大的趋势逐渐减缓。当功率升至  $75 \text{ W}$  时,如图 6(d)所示,金属飞溅现象加剧,飞溅的液滴会落在凹坑内部和凸起上方,增大了表面的起伏程度,此时粗糙度  $S_a$  为  $1.636 \mu\text{m}$ 。

图 7 为不同扫描速度激光清洗后铝合金的表面形貌,功率为  $45 \text{ W}$ ,线间距为  $0.04 \text{ mm}$ 。图 8 为不同

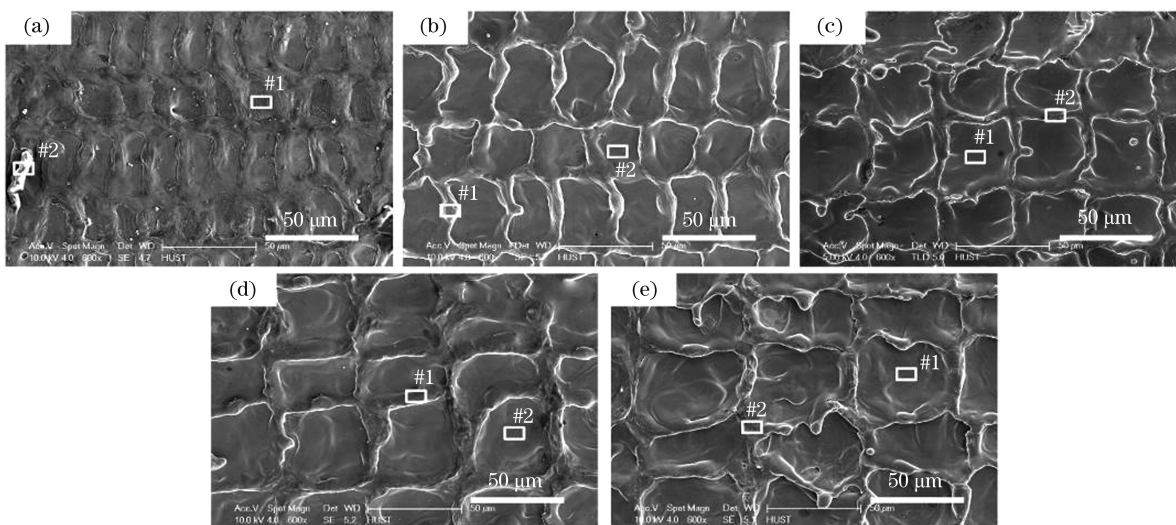


图 7 不同扫描速度激光清洗后铝合金的表面形貌。(a)  $2000 \text{ mm/s}$ ; (b)  $3000 \text{ mm/s}$ ; (c)  $4000 \text{ mm/s}$ ; (d)  $5000 \text{ mm/s}$ ; (e)  $6000 \text{ mm/s}$

Fig. 7 Surface morphology of 6061 aluminum alloy after laser cleaning with different scanning speed. (a)  $2000 \text{ mm/s}$ ; (b)  $3000 \text{ mm/s}$ ; (c)  $4000 \text{ mm/s}$ ; (d)  $5000 \text{ mm/s}$ ; (e)  $6000 \text{ mm/s}$

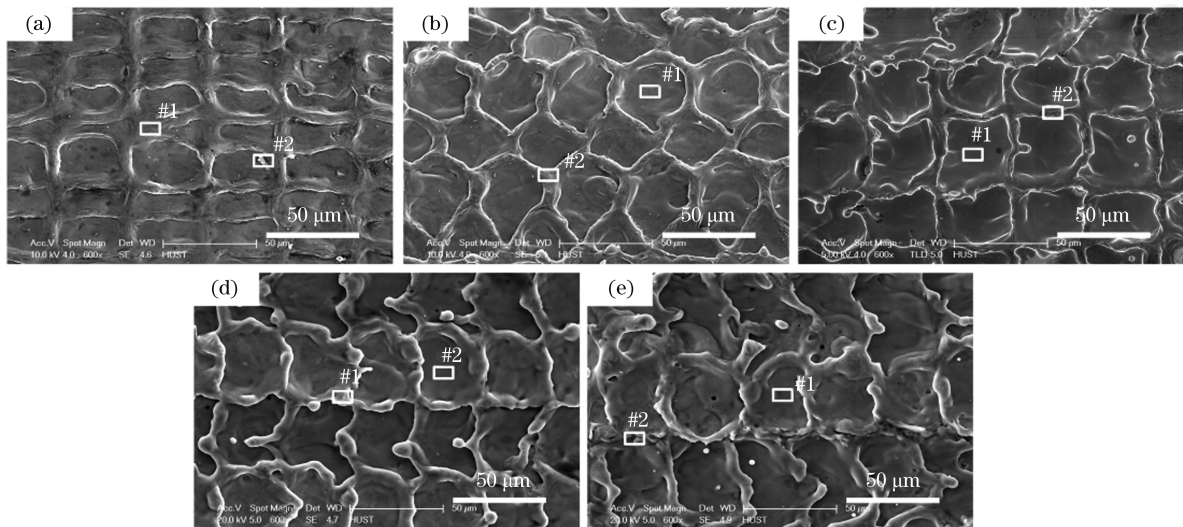


图 8 不同线间距激光清洗后 6061 铝合金的表面形貌。(a) 0.02 mm; (b) 0.03 mm; (c) 0.04 mm; (d) 0.05 mm; (e) 0.06 mm

Fig. 8 Surface morphology of 6061 aluminum alloy after laser cleaning with different line spacing. (a) 0.02 mm; (b) 0.03 mm; (c) 0.04 mm; (d) 0.05 mm; (e) 0.06 mm

线间距激光清洗后铝合金的表面形貌,功率为 45 W,扫描速度为 4000 mm/s。由于扫描速度和线间距均改变相邻激光光斑间距,故二者表面形貌的变化呈现相似的规律。当扫描速度为 2000 mm/s,线间距为 0.02 mm 时,表面比较平坦,凹坑的搭接痕迹不明显。随着扫描速度和线间距的增加,可以明显

看到排布规律的凹坑形貌,且形貌起伏程度增大。

图 9 为粗糙度随扫描速度和线间距的变化情况。从图中可以看出,二者均呈现先增大后减小的变化趋势,这与激光清洗过程中相邻凹坑形貌搭接有关。当扫描速度为 6000 mm/s,线间距为 0.06 mm 时,如图10(a)所示,相邻激光光斑的大间距导致凹

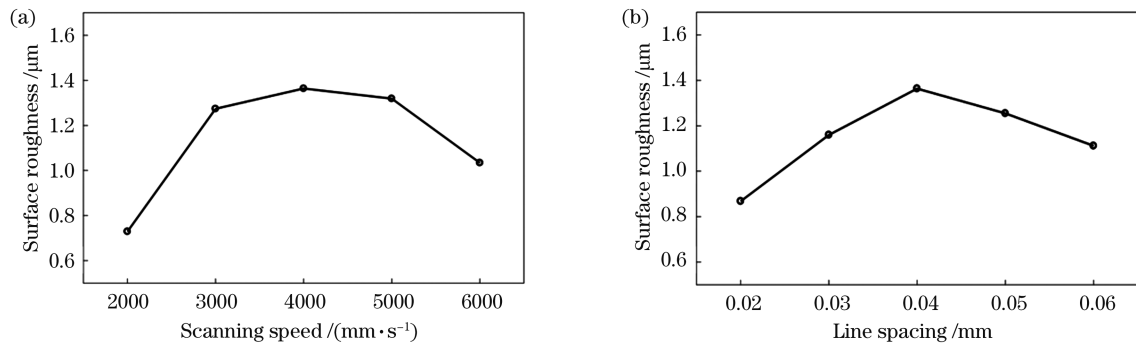


图 9 不同扫描速度和线间距激光清洗后铝合金表面粗糙度。(a)扫描速度;(b)线间距

Fig. 9 Surface roughness of 6061 aluminum alloy after laser cleaning with different scanning speed and line spacing. (a) Scanning speed; (b) line spacing

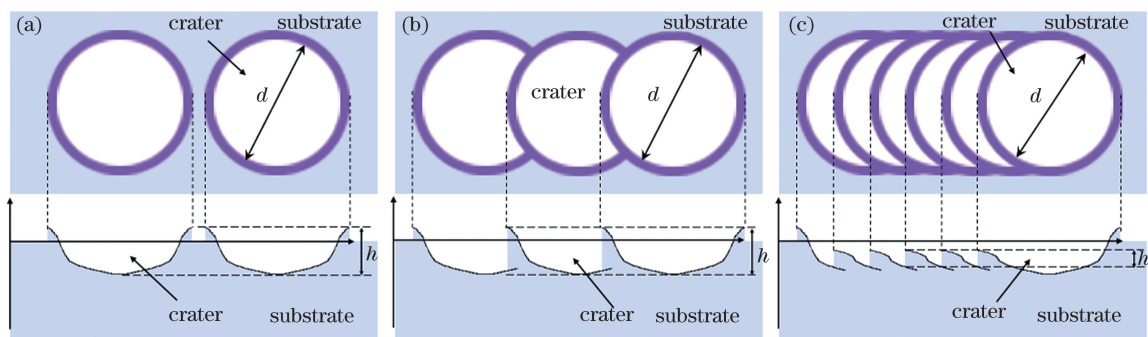


图 10 表面形貌随光斑间距的变化过程。(a)~(c)阶段 1~阶段 3

Fig. 10 Change process of surface morphology varying with spot spacing. (a)~(c) Stage 1~stage 3

坑形貌无法形成搭接,单位面积内凹坑形貌的数目较少,局部区域仍处于平坦的状态,此时粗糙度没有达到最大。当扫描速度为 3000~5000 mm/s,线间距为 0.03~0.05 mm 时,如图 10(b)所示,相邻的凹坑实现了较小程度的搭接,单位面积内的凹坑数目增多,粗糙度相应增大。当扫描速度为 2000 mm/s,线间距为 0.02 mm 时,如图 10(c)所示,相邻的凹坑实现了高程度的搭接,第 2 个凹坑的环状凸起已覆盖在第 1 个凹坑的最低处,形貌高低

起伏间距减小,粗糙度降低。

### 3.2 6061 铝合金激光清洗工艺窗口的建立

铝合金表面氧化层的主要成分为  $Al_2O_3 \cdot 3H_2O$ ,表面氧元素的含量可作为激光清洗效果的评价指标。采用 EDS 测试了不同工艺参数激光清洗后铝合金表面元素含量,每种工艺参数下检测 2 个不同的样本点以减小实验误差,检测位置如图 3、图 7 和图 8 中矩形线框所示,测试元素为 O、Al、Mg 和 Si,检测结果如表 2、表 3 和表 4 所示。

表 2 不同功率激光清洗后铝合金表面微区元素质量分数

Table 2 Mass fraction of elements in micro-area on surface of aluminum alloy after laser cleaning with different power unit: %

Element	15 W		30 W		45 W		60 W		75 W	
	#1	#2	#1	#2	#1	#2	#1	#2	#1	#2
O	7.28	1.68	0.48	0.60	0.86	0.93	0.78	1.11	2.90	4.10
Mg	4.70	1.95	1.62	1.49	1.52	1.55	1.47	1.67	1.77	3.37
Al	87.80	95.42	97.29	97.39	97.10	97.02	97.19	96.47	94.68	92.53
Si	0.22	0.95	0.62	0.51	0.52	0.50	0.56	0.75	0.65	0.00

表 3 不同扫描速度激光清洗后铝合金表面微区元素质量分数

Table 3 Mass fraction of elements in micro-area on surface of aluminum alloy after laser cleaning with different scanning speed unit: %

Element	2000 mm/s		3000 mm/s		4000 mm/s		5000 mm/s		6000 mm/s	
	#1	#2	#1	#2	#1	#2	#1	#2	#1	#2
O	5.61	23.44	0.74	0.57	0.86	0.93	0.00	1.10	0.49	4.60
Mg	3.51	2.48	1.50	4.74	1.52	1.55	0.11	1.55	0.56	4.56
Al	90.54	70.49	97.22	94.35	97.10	97.02	99.89	96.43	98.30	90.14
Si	0.35	3.58	0.53	0.34	0.52	0.50	0.00	0.91	0.65	0.69

表 4 不同线间距激光清洗后铝合金表面微区元素质量分数

Table 4 Mass fraction of elements in micro-area on surface of aluminum alloy after laser cleaning with different line spacing unit: %

Element	0.02 mm		0.03 mm		0.04 mm		0.05 mm		0.06 mm	
	#1	#2	#1	#2	#1	#2	#1	#2	#1	#2
O	3.17	14.45	0.00	0.94	0.86	0.93	0.00	1.05	0.87	7.99
Mg	4.26	4.02	4.15	3.85	1.52	1.55	3.89	4.27	4.24	4.84
Al	92.52	81.08	95.85	95.13	97.10	97.02	96.11	94.59	94.81	86.87
Si	0.06	0.46	0.00	0.08	0.52	0.50	0.00	0.09	0.08	0.30

从表 2 中可以看出:平均功率为 15 W 时,无法完全去除表面的氧化层;而功率为 75 W 时,出现了严重的二次氧化。当扫描速度为 2000 mm/s,线间距为 0.02 mm 时,相邻光斑能量的热积累会导致严重的氧化。而扫描速度为 6000 mm/s,线间距为 0.06 mm 时,相邻光斑的交界处仍残留有氧化层。

基于文献[15-17]的研究结果,以氧元素含量达到 2%以下作为指标,建立了 6061 铝合金表面自然氧化层激光清洗工艺窗口,具体参数为平均功率为 30~60 W,扫描速度为 3000~5000 mm/s,线间距为 0.03~0.05 mm。

## 4 工艺参数优化

### 4.1 面向粗糙度的 6061 铝合金激光清洗响应面模型的构建

粗糙度的变化显著影响铝合金的后续加工(如

焊接、涂装等)。建立工艺窗口,采用 Box-Behnken 实验设计方法构建粗糙度变化的响应面函数(即激光清洗后 6061 铝合金的表面粗糙度与脉冲激光的平均功率、扫描速度、线间距之间的函数关系式),实验结果如表 5 所示。

表 5 6061 铝合金激光清洗实验设计及粗糙度测试结果

Table 5 Experimental design and roughness test results of 6061 aluminum alloy using laser cleaning

No.	Laser power		Scanning speed		Line spacing		Surface roughness / $\mu\text{m}$
	Level	Value /W	Level	Value /( $\text{mm}\cdot\text{s}^{-1}$ )	Level	Value /mm	
1	-1	30	0	4000	-1	0.03	1.048
2	1	60	-1	3000	0	0.04	1.377
3	1	60	1	5000	0	0.04	1.586
4	0	45	1	5000	1	0.05	1.176
5	0	45	0	4000	0	0.04	1.364
6	1	60	0	4000	-1	0.03	1.296
7	-1	30	0	4000	1	0.05	0.957
8	-1	30	-1	3000	0	0.04	1.063
9	0	45	0	4000	0	0.04	1.338
10	-1	30	1	5000	0	0.04	0.995
11	0	45	0	4000	0	0.04	1.349
12	0	45	-1	3000	-1	0.03	1.024
13	1	60	0	4000	1	0.05	1.480
14	0	45	-1	3000	1	0.05	1.190
15	0	45	1	5000	-1	0.03	1.294

对实验数据进行拟合,采用如(3)式所示的二次多项式模型作为实际函数的近似,最终得出的 6061 铝合金经激光清洗后表面粗糙度 Sa 的二阶响应面模型方程为

$$R_{\text{Sa}} = -2.22 - 8.67 \times 10^{-3} \times P + 6.03 \times 10^{-4} \times$$

$$v + 105.27 \times l_y + 4.62 \times 10^{-6} \times P \times v + 0.46 \times P \times l_y - 7.1 \times 10^{-3} \times v \times l_y - 1.57 \times 10^{-4} \times P^2 - 5.97 \times 10^{-8} \times v^2 - 1196.67 \times l_y^2. \quad (4)$$

根据概率统计知识,该二阶响应面模型的方差分析结果如表 6 所示。

表 6 激光清洗铝合金表面粗糙度的二阶响应面模型的方差分析

Table 6 Variance analysis of the second-order response surface model of aluminum alloy surface roughness after laser cleaning

Source	Sum of squares	Degree of freedom	Mean square	F	$P_F$	Significance
Model	0.50	9	0.055	61.33	0.0001	Significant
$P$	0.35	1	0.35	390.88	<0.0001	
$v$	0.020	1	0.020	21.93	0.0054	
$l_y$	$2.485 \times 10^{-3}$	1	$2.485 \times 10^{-3}$	2.77	0.1571	
$P \times v$	0.019	1	0.019	21.35	0.0057	
$P \times l_y$	0.019	1	0.019	21.05	0.0059	
$v \times l_y$	0.020	1	0.020	22.45	0.0052	
$P^2$	$4.631 \times 10^{-3}$	1	$4.631 \times 10^{-3}$	5.16	0.0724	
$v^2$	0.013	1	0.013	14.63	0.0123	
$l_y^2$	0.053	1	0.053	58.86	0.0006	
Residual	$4.491 \times 10^{-3}$	5	$8.983 \times 10^{-4}$			
Lack of fit	$4.151 \times 10^{-3}$	3	$1.384 \times 10^{-3}$	8.12	0.1116	Not significant
Pure error	$3.407 \times 10^{-4}$	2	$1.703 \times 10^{-4}$			
Sum	0.50	14				

选定显著性水平  $\alpha = 0.05$ 。从表 6 中可以看出:模型的  $P_F$  值为 0.0001,表明此响应面近似函数模型的显著性达到了要求;失拟项的  $P_F$  值为 0.1116,表明影响 6061 铝合金粗糙度的其他因素可以忽略。根据方差分析结果发现,对于激光平均功率、扫描速度和线间距这 3 个工艺参数,对粗糙度显著性的影响顺序依次为平均功率、扫描速度、线间距。

#### 4.2 6061 铝合金激光清洗工艺参数优化及清洗效果验证

对(4)式响应面函数模型求极值,可获得 6061 铝合金经激光清洗后粗糙度达到最大时的工艺参数,如表 7 所示。理论求得的最优工艺参数为激光功率 60 W,扫描速度 4950 mm/s,线间距 0.041 mm,粗糙度  $S_a$  为  $1.584 \mu\text{m}$ 。为了验证优化结果的准确性,进行了 3 次验证实验,验证结果如表 7 所示。考虑到实验误差,基于此响应面函数模型优化的工艺参数结果具有较高的可信度。

图11为激光功率为60 W,扫描速度为4950 mm/s,

线间距为 0.04 mm 时的 6061 铝合金表面形貌。从图中可以看出,凹坑形貌规律地排布在铝合金表面,且无金属飞溅。测试了凹坑内部(#1处)和环状凸起(#2处)的元素相对含量,如图 12 所示,图中横坐标表示元素的 X 射线能量,纵坐标表示 X 射线计数,氧元素质量分数分别为 0.76%、0.99%,此表面状态已满足铝合金工业应用需求。

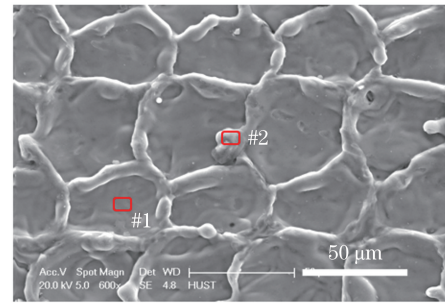


图 11 功率 60 W,扫描速度 4950 mm/s,线间距 0.04 mm 时 6061 铝合金的表面形貌

Fig. 11 Surface morphology of 6061 aluminum alloy when power is 60 W, scanning speed is 4950 mm/s, and line spacing is 0.04 mm

表 7 6061 铝合金激光清洗最优工艺

Table 7 Optimal laser cleaning process for 6061 aluminum alloy

Verification experiment	Laser power /W	Scanning speed / $(\text{mm}\cdot\text{s}^{-1})$	Line spacing /mm	Roughness / $\mu\text{m}$
1	60	4900	0.04	1.584
2	60	4950	0.04	1.592
3	60	5000	0.04	1.580
Theoretical value	60	4950	0.041	1.584

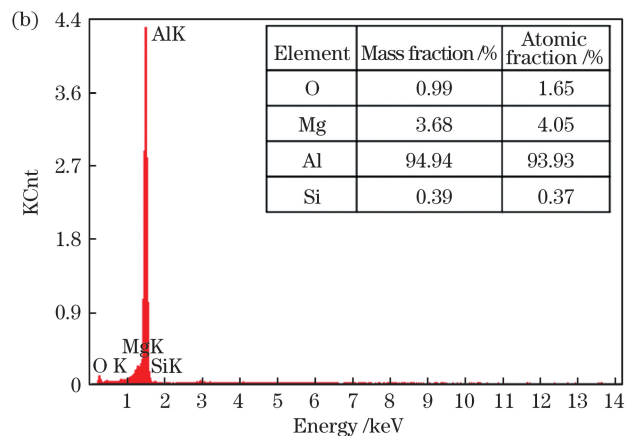
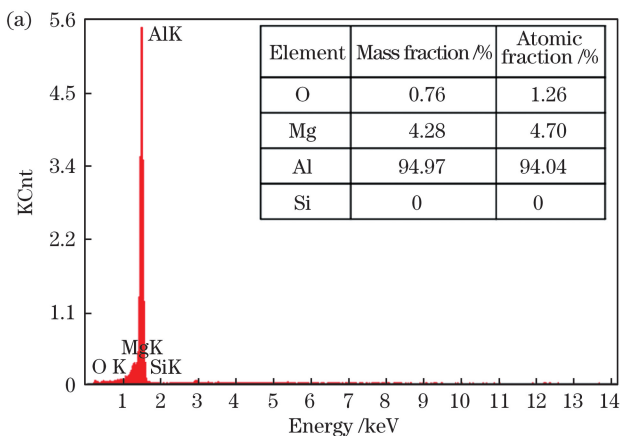


图 12 功率为 60 W,扫描速度为 4950 mm/s,线间距为 0.04 mm 时,6061 铝合金的表面元素相对含量。(a)位置 #1 处; (b)位置 #2 处

Fig. 12 Relative content of surface elements of 6061 aluminum alloy when power is 60 W, scanning speed is 4950 mm/s, and line spacing is 0.04 mm. (a) Location #1; (b) location #2

## 5 结 论

研究了激光清洗对 6061 铝合金表面形貌的影

响规律,建立了激光清洗 6061 铝合金表面自然氧化层的工艺窗口。基于此窗口,构建了 6061 铝合金表面粗糙度变化的函数模型,并对工艺参数进行进一

步优化。得出的主要结论如下。

1) 平均功率影响凹坑形貌的尺寸变化,进而改变表面粗糙度。在扫描速度为 4000 mm/s,线间距为 0.04 mm 时,当功率由 15 W 升高到 75 W,粗糙度 Sa 由 0.608  $\mu\text{m}$  增大至 1.636  $\mu\text{m}$ 。

2) 扫描速度和线间距影响相邻凹坑的搭接形貌,进而改变粗糙度。随着扫描速度和线间距的升高,粗糙度呈现先增大后减小的趋势。功率为 45 W 时,在扫描速度为 4000 mm/s,线间距为 0.04 mm 处,粗糙度 Sa 最大为 1.364  $\mu\text{m}$ 。

3) 根据元素能谱测试结果发现,激光清洗 6061 铝合金表面自然氧化层的工艺参数窗口为平均功率为 30~60 W,扫描速度为 3000~5000 mm/s,线间距 0.03~0.05 mm。

4) 在此工艺窗口内,建立了 6061 铝合金表面粗糙度变化的响应面函数模型,表面粗糙度达到最大时的工艺参数为平均功率为 60 W,扫描速度为 4950 mm/s,线间距为 0.041 mm,粗糙度 Sa 为 1.584  $\mu\text{m}$ 。元素能谱测试结果显示,以此工艺参数进行激光清洗后,表面氧元素的质量分数低于 1%,满足工业应用需求。

### 参 考 文 献

- [1] Zheng H, Zhao X Y. Lightweight automobile and application of aluminum alloys in modern automobile production [J]. *Forging & Stamping Technology*, 2016, 41(2): 1-6.  
郑晖, 赵曦雅. 汽车轻量化及铝合金在现代汽车生产中的应用 [J]. *锻压技术*, 2016, 41(2): 1-6.
- [2] Yu Z H. Research on microstructure and mechanical properties of friction stir welded joints for 7075 high strength aluminum alloy [D]. Guangzhou: South China University of Technology, 2020.  
俞宗华. 7075 高强铝合金搅拌摩擦焊工艺及接头组织和力学性能研究 [D]. 广州: 华南理工大学, 2020.
- [3] Chen Y M. Research on pre-welding laser cleaning of aluminum alloy and evaluation [D]. Wuhan: Huazhong University of Science and Technology, 2018.  
陈一鸣. 铝合金焊前激光清洗工艺及评估 [D]. 武汉: 华中科技大学, 2018.
- [4] Wang Q, Guan Y C, Cong B Q, et al. Laser cleaning of commercial Al alloy surface for tungsten inert gas welding [J]. *Journal of Laser Applications*, 2016, 28(2): 022507.
- [5] AlShaer A W, Li L, Mistry A. The effects of short pulse laser surface cleaning on porosity formation and reduction in laser welding of aluminium alloy for automotive component manufacture [J]. *Optics & Laser Technology*, 2014, 64: 162-171.
- [6] Yousaf D, Bashir S, Akram M, et al. Laser irradiation effects on the surface, structural and mechanical properties of Al-Cu alloy 2024 [J]. *Radiation Effects and Defects in Solids*, 2014, 169(2): 144-156.
- [7] Zheng B X, Jiang G D, Wang W J, et al. Surface ablation and threshold determination of AlCu<sub>4</sub>SiMg aluminum alloy in picosecond pulsed laser micromachining [J]. *Optics & Laser Technology*, 2017, 94: 267-278.
- [8] Zhu G D, Wang S R, Cheng W, et al. Investigation on the surface properties of 5A12 aluminum alloy after Nd:YAG laser cleaning [J]. *Coatings*, 2019, 9(9): 578.
- [9] Shi T Y, Wang C M, Mi G Y, et al. A study of microstructure and mechanical properties of aluminum alloy using laser cleaning [J]. *Journal of Manufacturing Processes*, 2019, 42: 60-66.
- [10] Zhang G X, Hua X M, Li F, et al. Effect of laser cleaning process parameters on the surface roughness of 5754-grade aluminum alloy [J]. *The International Journal of Advanced Manufacturing Technology*, 2019, 105(5/6): 2481-2490.
- [11] Zhang G X, Hua X M, Huang Y, et al. Investigation on mechanism of oxide removal and plasma behavior during laser cleaning on aluminum alloy [J]. *Applied Surface Science*, 2020, 506: 144666.
- [12] Liu B W, Mi G Y, Wang C M. Study on surface state and thermophysical properties of TA15 alloy by laser ablation [J]. *Journal of Manufacturing Processes*, 2021, 62: 483-490.
- [13] Liu B W, Mi G Y, Wang C M. Research on grain refinement and wear behavior of micro-remelted TA15 alloy surface by laser cleaning [J]. *Materials Chemistry and Physics*, 2021, 259: 124022.
- [14] Liu B W, Mi G Y, Wang C M. Study on the morphology and microstructure of 5A06 alloy by high-pulse-frequency pulsed laser micro polishing [J]. *Materials Chemistry and Physics*, 2020, 255: 123500.
- [15] Wang G. Study on effect of pulse laser cleaning on surface morphology and welding quality of aluminum alloy [D]. Changsha: Hunan University, 2018.  
王刚. 脉冲激光清洗对铝合金表面形貌及焊接质量的影响研究 [D]. 长沙: 湖南大学, 2018.
- [16] Dong W Q. Influence of removal of anodic oxide film from 5083 aluminum alloy by laser cleaning on the welding quality of laser welding [D]. Wuhan: Hubei University of Technology, 2018.  
董文祺. 激光清洗 5083 铝合金阳极氧化膜对激光焊

- 接质量的影响[D]. 武汉: 湖北工业大学, 2018.
- [17] Huang J Y. Research on pretreatment mechanism and experiment of 6061 aluminum alloy by nanosecond laser before welding [D]. Zhenjiang: Jiangsu University, 2018.  
黄建宇. 6061 铝合金焊接前纳秒激光表面预处理机制与实验研究[D]. 镇江: 江苏大学, 2018.
- [18] Ang L K, Lau Y Y, Gilgenbach R M, et al. Analysis of laser absorption on a rough metal surface [J]. *Applied Physics Letters*, 1997, 70(6): 696-698.
- [19] Wang X, Xu M Y, Wang Z W, et al. Properties of jet-plated Ni coating on Ti alloy ( $Ti_6Al_4V$ ) with laser cleaning pretreatment[J]. *Metals*, 2019, 9(2): 248.
- [20] Maroofi A, Navab S N, Ghomi H. Atmospheric air plasma jet for improvement of paint adhesion to aluminum surface in industrial applications [J]. *International Journal of Adhesion and Adhesives*, 2020, 98: 102554.
- [21] Luo A H. Study on heat flow coupling and heat convecting of resistance spot welding electrode [D]. Shanghai: Shanghai Jiao Tong University, 2007.  
罗爱辉. 电阻点焊电极热流耦合分析与对流传热特性研究[D]. 上海: 上海交通大学, 2007.
- [22] Zhang X Y. Research on failure mechanism and control methods of interfacial fracture mode for dual phase steel welds[D]. Shanghai: Shanghai Jiao Tong University, 2008.  
张小云. 双相钢点焊熔核界面撕裂失效机理与控制方法研究[D]. 上海: 上海交通大学, 2008.
- [23] Guo L Y, Geng S N, Gao X S, et al. Numerical simulation of heat transfer and fluid flow during nanosecond pulsed laser processing of  $Fe_{78}Si_9B_{13}$  amorphous alloys [J]. *International Journal of Heat and Mass Transfer*, 2021, 170: 121003.

## Experimental Study on Surface Morphology Changes of Aluminum Alloy Using Laser Cleaning and Optimization of Process Parameters

Li Yuqiang<sup>1</sup>, Guo Lingyu<sup>1</sup>, Jiang Ping<sup>1\*</sup>, Geng Shaoning<sup>1</sup>, Wang Chunming<sup>2</sup>,  
Gao Song<sup>1</sup>, Han Chu<sup>1</sup>

<sup>1</sup> School of Mechanical Science and Engineering, Huazhong University of Science and Technology, Wuhan, Hubei 430074, China;

<sup>2</sup> School of Materials Science and Engineering, Huazhong University of Science and Technology, Wuhan, Hubei 430074, China

### Abstract

**Objective** Aluminum alloy is widely used in aerospace, automobile manufacturing, and other fields. An oxide layer easily forms on the surface of aluminum alloy, which seriously affects the welding quality. As a result, there is an urgent need for high-quality removal technology. Compared with traditional cleaning methods, laser cleaning has obvious advantages in cleaning effect and process flexibility. Laser cleaning changes the surface morphology and roughness of aluminum alloy and seriously affects subsequent processing, such as welding and painting. At present, most researchers have only compared the differences in the surface morphology of aluminum alloy before and after laser cleaning. However, they have not systematically explained the reasons for the changes in morphology and roughness. Therefore, this article investigates aluminum alloy to explore the correlation between laser cleaning process parameters and surface morphology and roughness. A laser cleaning process window for the natural oxide layer on the surface of 6061 aluminum alloy was established. Based on this window, the process parameters were optimized to maximize surface roughness, which provides process guidance for adjusting the surface morphology of aluminum alloy.

**Methods** This article uses a pulsed laser with a maximum power of 100 W (YDFLP-100-LM1) for laser cleaning experiments. The laser wavelength is 1064 nm, and the spot diameter is 70  $\mu\text{m}$ . In this article, the fixed pulse width is 100 ns and the repetition frequency is 100 kHz. This paper uses 6061 aluminum alloy with a thickness of 2 mm as the substrate. Single-factor experiments are used to study the influence of average power, scanning speed, and line spacing on the laser cleaning effect. After laser cleaning, the FEI Sirion 200 scanning electron microscope was used to characterize the surface morphology, the energy spectrometer was utilized to test the changes in surface element content, and the OLYMPUS DSX 510 three-dimensional microscope was employed to test the changes in surface

roughness. Furthermore, this paper uses the response surface analysis method to optimize the process parameters within the established process window.

**Results and Discussions** When the average power is 15 W, only small craters are formed on the surface. Most areas do not have ablation craters of the same size. With an increase in power, apparent crater overlap morphology is gradually formed. When the power is increased to 75 W, the laser energy is too large, resulting in severe thermal ablation, and a large amount of metal splash destroys the lap morphology of the craters. As the power increases from 15 W to 75 W, the roughness increases from  $0.608\ \mu\text{m}$  to  $1.636\ \mu\text{m}$ . Consequently, the variation in aluminum alloy surface morphology with power can be divided into four stages (Fig. 6). Since the scanning speed and line spacing change the positioning between adjacent laser spots, the changes in their surface topography exhibit similar laws. When the scanning speed is 2000 mm/s, and the line spacing is 0.02 mm, the surface is relatively flat, and the overlap marks of the craters are not noticeable. With increased scanning speed and line spacing, the crater morphology with regular arrangement can be observed with an increased degree of morphology fluctuation. As the scanning speed and line spacing increase, the roughness first increases and then decreases. As a result, the change in aluminum alloy surface morphology can be divided into three stages (Fig. 10). Through the element content test, with the oxygen content below 2% as the indicator, the laser cleaning process window for the natural oxide layer on the surface of 6061 aluminum alloy is established as follows: the average power is between 30 W and 60 W, the scanning speed is between 3000 mm/s and 5000 mm/s, and the line spacing is between 0.03 mm and 0.05 mm. Based on the response surface analysis method, the function of the surface roughness change after laser cleaning is formulated. According to the analysis of variance results, average power, scanning speed, and line spacing influence roughness in the increasing order of significance. The optimal process parameters obtained theoretically include a laser power of 60 W, a scanning speed of 4950 mm/s, and a line spacing of 0.041 mm. The three verification experiments confirm that the results have high credibility.

**Conclusions** In this paper, the influence of laser cleaning on the surface morphology of 6061 aluminum alloy was studied. The average power affects the crater morphology, which in turn changes the surface roughness. As the laser power increases, the roughness gradually increases. The scanning speed and line spacing affect the lap morphology of adjacent craters, thereby changing the roughness. As the scanning speed and line spacing increase, the roughness first increases and then decreases. According to the results of the elemental energy spectrum test, it is found that the process parameter window for laser cleaning the natural oxide layer on the surface of 6061 aluminum alloy is as follows: the average power is between 30 W and 60 W, the scanning speed is between 3000 mm/s and 5000 mm/s, and the line spacing is between 0.03 mm and 0.05 mm. Based on this window, a function model for the surface roughness change of 6061 aluminum alloy was established. The process parameters are as follows when the surface roughness reaches the maximum: the average power is 60 W, the scanning speed is 4950 mm/s, and the line spacing is 0.041 mm. Elemental energy spectrum test results demonstrate that the relative content of surface oxygen is less than 1%, which meets industrial application requirements.

**Key words** laser technology; laser manufacturing; laser cleaning; aluminum alloy; surface morphology; roughness; process parameter optimization

**OCIS codes** 140.3390; 140.3510; 140.3538